Reproduction and analysis of: R-matrix type parametrization of the Jost function for extracting the resonance parameters from scattering data

Juliana Prada Suarez (jupradas@unal.edu.co)
Cristian Eduardo Martínez Torres (crmartinezto@unal.edu.co)

Abstract This document presents the development and outcomes of the final project for the course "Introduction to the Theory of Nuclear Reactions." Our primary goal was to reproduce the key results of a published article [7] by implementing the methodologies it described. The project successfully achieved this objective: the extracted resonance parameters closely match both the theoretical predictions and the values reported in the original work, and in a few cases they outperform the results found in the article. Along the way, significant insight was gained into advanced theories and techniques in scattering theory, exploring approaches beyond those covered in the course curriculum yet aligned with its learning objectives.

1 Introduction

In nuclear physics, scattering processes are one of the most studied phenomena, as they provide deep understanding in the nature of nuclear interactions. Experimentally, researchers measure cross-section data, which encapsulate the physical dynamics of interest. One intrinsic phenomenon in scattering processes is the formation of resonances. These states are quasi-bound states (states confined with positive energy), which can be characterized by their resonance energy E_r —the energy at which they manifest— and their width Γ —related to the half-life of the resonant state—.

Resonances reveal themselves as irregularities in the cross-section curves. In a few cases, they emerge as pronounced, bell-shaped peaks, enabling direct determination of resonance parameters with good precision. However, in most cases, they manifest only as subtle deviations from the monotonic trend of the cross section, making both identification and parameter determination challenging. Various approaches exist for extracting resonance parameters from experimental data. Most of these methods rely on the fact that each resonance corresponds to a pole of the S-matrix at a complex energy [1], those poles have the following mathematical expression

$$E = E_r - \frac{i}{2}\Gamma$$

Naturally, all these methods are grounded in the S-matrix and its use in fitting experimental data. What ultimately distinguishes each method is how they parametrize the S-matrix to ensure compatibility with analytic continuation into the complex plane. Thus, the choice of an appropriate functional form for this parametrization becomes the determining factor in a method's success. Since this article focuses on two specific approaches: the traditional Jost function method and the R-matrix method, our analysis will likewise be restricted to these two cases.

Regarding the Jost function method, we must acknowledge an important advantage: in the expressions defining these functions, most factors are previously known and are analytic. The remaining unknown factors, which correspond to the adjustable parameters, are guaranteed to be single-valued and analytic. It has been proposed [5] that these unknown factors can be approximated as polynomials in the variable $(E - E_0)$, derived from a Taylor series expansion around E_0, where the coefficients of each term become the fitting parameters. While this method has been successfully tested for extracting resonance parameters [8], it requires a substantially large number of fitting parameters to achieve reliable results.

On the other hand, the R-matrix method also constitutes a reliable approach for obtaining scattering matrix poles and, consequently, resonance parameters.

$$R_\ell(E, B_R) = \sum_{n=1}^{N} \frac{[\gamma_{n\ell}(B_R)]^2}{E_{n\ell} - E} \tag{1}$$

Its implementation via the phenomenological R-matrix (1) requires fewer fitting parameters than the Jost function method, representing a clear advantage. However, it exhibits a strong dependence on the channel radius (the radial coordinate value beyond which nuclear potential effects become negligible), as demonstrated in several academic scenarios. This channel radius choice is arbitrary with no selection criteria to ensure accuracy. Furthermore, when the S-matrix parametrization derives from a polynomial expansion (as the R-matrix adopts a polynomial-sum functional form), the resulting zeros may correspond to nonphysical resonances in the system [3].

As evidenced by the description of both methods, the authors faced the need to overcome the limitations of each approach while simultaneously boosting their advantages. Given this context, proposing a hybrid method that exploits these strengths while mitigating or eliminating the drawbacks appears to be a logical solution. This is precisely the contribution of the article. Consequently, our work in this project will focus on understanding the theoretical background of the proposed method and reproducing the results obtained in the study through its implementation.

Final preliminary considerations include the authors' exclusive focus on the single-channel problem, though we will later address multi-channel applications in the conclusions. The experimental data being fitted consisted of artificially generated data derived from the Noro-Taylor potential with a Coulomb tail, a standard test case for nuclear scattering methods. This potential was implemented within the two-body scattering problem solution method based on the calculation of Jost functions.

2 Theoretical background

The Jost functions have been extensively documented in the literature [1, 2, 4] and have served as the basis for numerous applications in scattering theory. Their mathematical derivation (both rigorous and physically consistent) is well established. These functions are defined through the regular solution of the radial Schrödinger equation and are formally characterized as the amplitudes of the incoming and outgoing Coulomb-Haenkel wave functions in the asymptotic behavior of this solution.

$$\phi_\ell(k, r \to \infty) \to \frac{1}{2}\left[H_\ell^{(+)}(\eta, kr) f_\ell^{\text{in}}(\eta, k) + H_\ell^{(-)}(\eta, kr) f_\ell^{(\text{out})}(\eta, k)\right]$$

As previously noted in the introduction, the functional form of the Jost functions is well-known, with explicitly known analytic factors, as will be demonstrated in what follows.

$$f_\ell^{(\text{in/out})}(E) = e^{\mp i\delta_\ell^c} k^\ell \left\{ \frac{k}{D_\ell(\eta, k)} A_\ell(E) - [M(k) \pm i] D_\ell(\eta, k) B_\ell(E) \right\}$$

Where

$$M(k) = \frac{2\eta\, h(\eta)}{C_0^2(\eta)}, \qquad D_\ell(\eta, k) = C_\ell(\eta) k^{\ell+1},$$

$$h(\eta) = \frac{1}{2}[\psi(1 + i\eta) + \psi(1 - i\eta)] - \ln\eta,$$

The pure Coulomb phase shift

$$\delta_\ell^c(\eta) = \frac{1}{2i} \ln\left(\frac{\Gamma(\ell + 1 + i\eta)}{\Gamma(\ell + 1 - i\eta)}\right),$$

The Coulomb barrier factor

$$C_\ell(\eta) = \frac{e^{-\pi\eta/2}}{\Gamma(\ell + 1)} \exp\left\{\frac{1}{2}[\ln\Gamma(\ell + 1 + i\eta) + \ln\Gamma(\ell + 1 - i\eta)]\right\} \tag{2}$$

And the Digamma function

$$\psi(z) = \frac{\Gamma'(z)}{\Gamma(z)}$$

The factors $A_\ell(E)$ and $B_\ell(E)$ were approximated by N terms of the Taylor expansions around a point E_0

$$A_\ell(E) \approx \sum_{n=0}^{N} a_n(\ell, E_0)(E - E_0)^n \tag{3}$$

$$B_\ell(E) \approx \sum_{n=0}^{N} b_n(\ell, E_0)(E - E_0)^n \tag{4}$$

Where the coefficients a_n and b_n are the fitting parameters. As can be inferred from expressions (3) and (4), the number of terms retained in the series expansion directly determines the method's accuracy. This presents a significant implementation limitation, as the need to optimize numerous parameters is impractical. To address this challenge, the authors propose replacing these series expansions with an alternative approach based on the R-matrix formalism.

The Jost functions admit a known representation in terms of the R-matrix [9], which we present below

$$f_\ell^{(\text{in/out})}(E) = \frac{\pm i\, e^{\pm i\delta_\ell}\, k^\ell}{Q_\ell(E, B_R)} \Big\{ H_\ell^{(\pm)}(\eta, ka) - \left[a \frac{d}{dr} H_\ell^{(\pm)}(\eta, kr)\Big|_{r=a} - B_R\, H_\ell^{(\pm)}(\eta, ka)\right] R_\ell(E, B_R) \Big\} \tag{5}$$

Where

$$Q_\ell(E, B_R) = \sum_{n=1}^{N} \frac{\lambda_{n\ell}(B_R)\gamma_{n\ell}(B_R)}{E_{n\ell} - E}$$

By performing a term-by-term comparison between (2) and (5), and expressing both the Q-matrix and the R-matrix as polynomial expansions, we derive two new expressions for the coefficients $A_\ell(E)$ and $B_\ell(E)$ corresponding to the paper's proposal

$$A_\ell(E) = \sum_{n=0}^{N} \alpha_{n\ell}\, \mathcal{P}_n(E) \tag{6}$$

$$B_\ell(E) = \sum_{n=0}^{N} \beta_{n\ell}\, \mathcal{P}_n(E) \tag{7}$$

Where

$$\mathcal{P}_n(E) = \frac{\mathcal{P}_0(E)}{E_{n\ell} - E}$$

$$\mathcal{P}_0(E) = \prod_{n=1}^{N} (E_{n\ell} - E)$$

3 Understanding the method

In experimental nuclear physics studies, researchers typically obtain a set of experimental total cross-section data points with their corresponding measurement uncertainties as a function of collision energies

$$\sigma_{\text{total}}(E_i) \pm \Delta_i$$

The next step involves parameterizing the functions (6) and (7) and substituting them into the S-matrix representation

$$S_\ell(E) = e^{2i\delta_\ell^c} \frac{kA_\ell(E) - [M(k) - i] D_\ell^2(\eta, k) B_\ell(E)}{kA_\ell(E) - [M(k) + i] D_\ell^2(\eta, k) B_\ell(E)}$$

The total cross-section is then calculated as the sum of all contributing partial cross-sections

$$\sigma_{\text{total}}(E) = \sum_{\ell=0}^{\ell_{\max}} \sigma_\ell(E)$$

$$\sigma_\ell(E) = \frac{\pi}{k^2}(2\ell + 1)|S_\ell(E) - 1|^2$$

Regarding our implementation, the first step in the paper's implementation was to generate the artificial experimental data

to be fitted. The total cross-section is computed using two-body scattering problem resolution methods when the functional form of the nuclear potential is known. For this particular case, the authors employed the Noro-Taylor potential with a Coulomb tail

$$V(r) = \frac{\hbar^2}{2\mu}\left(7.5r^2e^{-r} + \frac{2k\eta}{r}\right)$$

The approach adopted in the article for obtaining the exact (theoretical) cross section is based on the direct calculation of the Jost functions. This method combines variable-constant techniques with complex coordinate rotation methods to solve the Schrödinger equation [6]. The authors selected this method as it eliminates the need for approximations, series expansions or variational procedures. Fundamentally, the technique involves performing a complex continuation of the radial coordinate and seeking solutions of the form (8) for the neighborhood of the origin, while employing solutions of the form (9) for large r values.

$$\Phi_\ell(k,r) = F_\ell(\eta,kr)A_\ell(\eta,k,x,\theta) + G_\ell(\eta,kr)B_\ell(\eta,k,x,\theta) \quad (8)$$

$$\Phi_\ell(k,r) = \frac{1}{2}\left[H_\ell^{(+)}(\eta,kr)\mathcal{F}_\ell^{(+)}(k,x,\theta) + H_\ell^{(-)}(\eta,kr)\mathcal{F}_\ell^{(-)}(k,x,\theta)\right] \quad (9)$$

This approach requires solving a system of two coupled first-order differential equations for each independent solution

$$\begin{aligned}\partial_x\mathcal{F}_\ell^{(+)}(k,x,\theta) = &-\frac{e^{i\theta}}{2ik}H_\ell^{(+)}(\eta,kr)V(r)\left[H_\ell^{(+)}(\eta,kr)\right.\\ &\left.\times\mathcal{F}_\ell^{(+)}(k,x,\theta) + H_\ell^{(-)}(\eta,kr)\mathcal{F}_\ell^{(-)}(k,x,\theta)\right]\end{aligned}$$

$$\begin{aligned}\partial_x\mathcal{F}_\ell^{(+)}(k,x,\theta) = &\frac{e^{i\theta}}{2ik}H_\ell^{(-)}(\eta,kr)V(r)\left[H_\ell^{(+)}(\eta,kr)\right.\\ &\left.\times\mathcal{F}_\ell^{(+)}(k,x,\theta) + H_\ell^{(-)}(\eta,kr)\mathcal{F}_\ell^{(-)}(k,x,\theta)\right]\end{aligned}$$

$$\begin{aligned}\partial_x A_\ell(\eta,k,x,\theta) = &\frac{e^{i\theta}}{k}G_\ell(\eta,kr)V(r)[F_\ell(\eta,kr)A_\ell(\eta,k,x,\theta)\\ &+ G_\ell(\eta,kr)B_\ell(\eta,k,x,\theta)]\end{aligned}$$

$$\begin{aligned}\partial_x B_\ell(\eta,k,x,\theta) = &-\frac{e^{i\theta}}{k}F_\ell(\eta,kr)V(r)[F_\ell(\eta,kr)A_\ell(\eta,k,x,\theta)\\ &+ G_\ell(\eta,kr)B_\ell(\eta,k,x,\theta)]\end{aligned}$$

It is necessary to document the challenges encountered during our implementation of the artificial experimental data generation. The coupled differential equation system for the two spatial regions (r ∈ [0,1] and r ∈ [1,30]) was solved numerically in Python using SciPy's Runge-Kutta method. However, we identified significant implementation issues, primarily due to the suboptimal optimization of Coulomb functions in the cmath library. Since the method's precision required over 300 integration points, each demanding computationally expensive Coulomb function evaluations, this limitation became critical. While switching programming languages could have mitigated these efficiency constraints, we ultimately decided to remain consistent with the project's objective of reproducing the proposed methodology.

For the fitting procedure of the 'experimental' data, we fitted 40 energy data points from 1.7 to 5 MeV. The optimization was performed using the MINUIT minimization routine in Python, where the fitting parameters were determined by minimizing the chi-squared statistic

$$\chi^2 = \sum_{i=1}^{N^{(\text{data})}}\left[\frac{\sigma_{\text{total}}(E_i) - \sigma_{\text{fit}}(E_i)}{\Delta_i}\right]^2$$

The resonance parameters are obtained by locating the zeros of the Jost functions, as calculated via equation (2), using numerical root-finding techniques, in our case: the Newton-Rhapson method.

Once again, it is important to address the implementation details of the fitting procedure. First, we verified the exactitude of the factors dominating the Jost functions by attempting to reproduce the curves obtained by the authors using their reported fitting parameters. During this validation process, we identified an error in equation (2), which was missing a crucial term responsible for the curve's dependence on partial wave variations. The corrected equation for this factor is presented below

$$\begin{aligned}C_\ell(\eta) = &\frac{1}{(2\ell+1)!!}\frac{e^{-\pi\eta/2}}{\Gamma(\ell+1)}\\ &\times\exp\left\{\frac{1}{2}[\ln\Gamma(\ell+1+i\eta) + \ln\Gamma(\ell+1-i\eta)]\right\}\end{aligned}$$

On the other hand, we identified an error in the definition of the Sommerfeld parameter, where an incorrect factor of 2 was included. This erroneous factor substantially affected the scaling of the theoretical curves

$$\eta = -\frac{1}{2k} \longrightarrow \eta = -\frac{1}{k}$$

In the following section, we present both the obtained cross-section curves and the extracted resonance parameters. These results are compared with theoretical predictions and the values reported in the original article.

4 Results

Application of the described methodology to the artificial experimental data derived from the article's graphical results yielded the total cross-section presented in 1a. From the fitting parameters obtained through this analysis, we computed the partial cross-sections for angular momentum states $l = 0$, $l = 1$, and $l = 2$, with the resulting curves and their exact theoretical counterparts displayed in 1b, 1c and 2, respectively. The determination of the Jost function zeros, obtained by substituting these parameters into its analytical expression, enabled extraction of the resonance energies and widths. The

complete set of results, including comparisons with both theoretical predictions and previously reported values, is tabulated in Table 1.

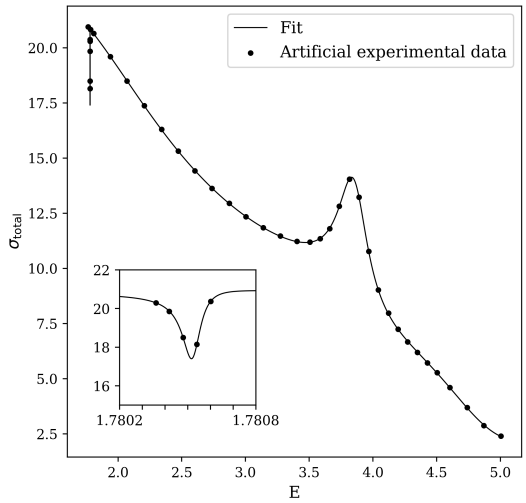

(a) Total cross-section data points and fitting curve

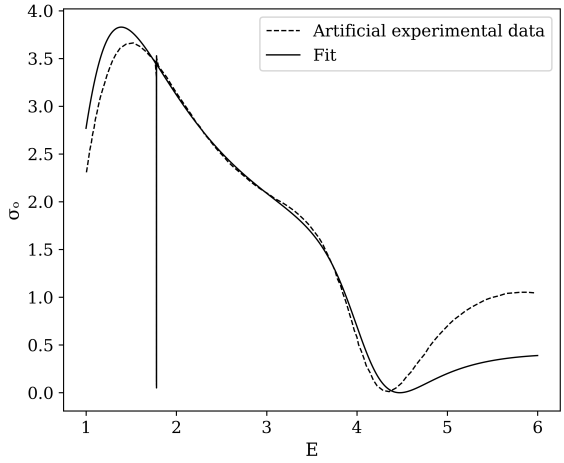

(b) Partial cross-section for $l = 0$

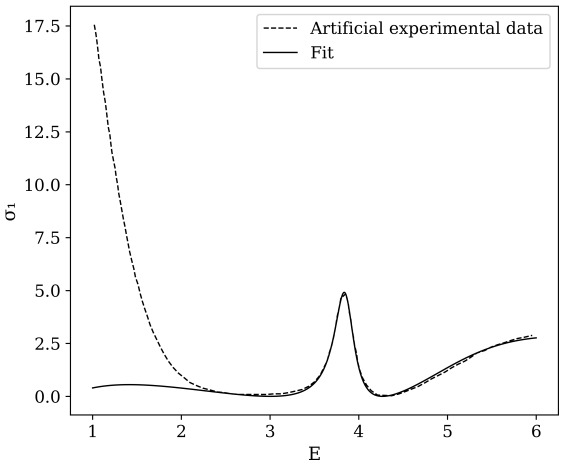

(c) Partial cross-section for $l = 1$

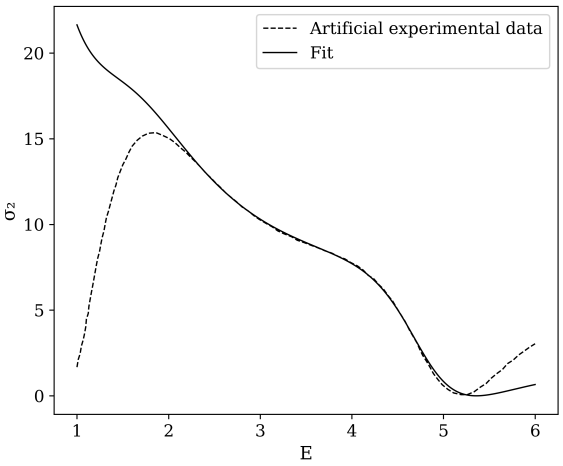

Figure 2: Partial cross-section for $l = 2$.

Resonance energies E_r

ℓ	Exact	Paper fit	Our fit
0	1.780524536	1.780524652	1.780524652
	4.101494947	4.100074051	4.091824032
1	3.848001634	3.854146542	3.854243692
2	4.900516145	4.802927949	4.793964753

Resonance widths Γ

ℓ	Exact	Paper fit	Our fit
0	9.5719×10^{-5}	9.6022×10^{-5}	9.6022×10^{-5}
	1.157254423	1.126491452	1.124152995
1	0.275384458	0.272421209	0.273634632
2	1.567507025	1.423821138	1.436464385

Table 1: Resonance parameters

5 Conclusions

Mainly due to the computational limitations of cmath's implementation of the Haenkel–Coulomb functions (specifically its inefficiency when performing large numbers of numerical calculations) it was not possible to reproduce the theoretical curve from the Noro–Taylor potential. Since evaluating these functions at many points is crucial for accurate results, it is reasonable to consider migrating to a more efficient programming language as C++ or FORTRAN. However, to preserve the purpose of this work (i.e., reproducing the new method) and because this is not directly related to the article's core focus, we decided to proceed with the following sections based on the provided exact graphs.

By thoroughly understanding the theoretical and computational framework proposed in the article, implementing the provided equations, and correcting certain factors that were missing compared to the literature, we successfully reproduced the method described by the authors. The associated fitting curves related to both the total and partial cross-section for the extracted artificial experimental dataset have proved to be indistinguishable from those presented in the paper. This result was obtained by the construction of a Python code which was also capable of extracting the resonance parameters within a satisfactory range, as evidenced by the percentage relative-error values. It is worth highlighting the efficiency of the MINUIT

minimization routine in fitting a large number of parameters within a short time frame.

From the results obtained, it is clear that the method outperforms its predecessors, fulfilling its objective of combining the advantages of both and solving (at least partially) their drawbacks. However, it must be taken into account that, although this approach is more efficient than the traditional Jost-function method (with Taylor-type expansions), it still involves a considerable number of parameters, which may grow with the complexity of the problem being solved. Additionally, there is a variable dependence on the values chosen to initialize the minimization process and on the "suspected" resonance energy values, which can affect its efficiency in some cases and its accuracy in others.

References

[1] L. F. Canto and M. S. Hussein. *Scattering Theory of Molecules, Atoms and Nuclei*. World Scientific, 2013.

[2] Michael G. Fuda and James S. Whiting. Generalization of the Jost Function and its Application to Off-Shell Scattering. *Phys. Rev. C*, 8(4):1255–1265, October 1973.

[3] Alexander Moroz and Andrey E. Miroshnichenko. On beautiful analytic structure of the S-matrix. *New Journal of Physics*, 21(10):103035, 2019.

[4] S. A. Rakityansky. *Jost Functions in Quantum Mechanics: A Unified Approach to Scattering, Bound, and Resonant State Problems*. Springer, Berlin, 2022.

[5] S. A. Rakityansky and N. Elander. Analytic structure of the multichannel Jost matrix for potentials with Coulombic tails. *Journal of Mathematical Physics*, 54(12):122112, 2013.

[6] S. A. Sofianos and S. A. Rakityansky. Exact method for locating potential resonances and Regge trajectories. *Journal of Physics A: Mathematical and General*, 30:3725–3737, 1997.

[7] P. Vaandrager, M. L. Lekala, and S. A. Rakityansky. R-matrix type parametrization of the Jost function for extracting the resonance parameters from scattering data. *European Physical Journal A*, 61:79, 2025.

[8] P. Vaandrager and S. A. Rakityansky. Extracting the resonance parameters from experimental data on scattering of charged particles. *International Journal of Modern Physics E*, 25(2):1650014, 2016.

[9] Paul Vaandrager, Jérémy Dohet-Eraly, and Jean-Marc Sparenberg. The Jost function and Siegert pseudostates from R-matrix calculations at complex wavenumbers. *arXiv preprint*, June 2023.